PROCEEDINGS OF THE YEREVAN STATE UNIVERSITY

Physical and Mathematical Sciences 2023, **57**(3), p. 101–110

P h y s i c s

THE RESONANT RESPONSE OF STRONGLY COUPLED NANORODS TO THE ELECTROMAGNETIC WAVE

D. A. MANUKYAN *

Chair of Radiophysics and Electronics, Institute of Physics, YSU, Armenia

The electromagnetic response of closely spaced nanorod dimers can be controlled via the modification of the nanoparticles interaction, caused by electron tunneling between them. The optical response to an intense external electromagnetic field of a system composed of two gold 230 *nm* long rods surrounded by air and separated by a gap of width 0.5 *nm* was analyzed. Using finite element method-based numerical simulations we show that the electron tunneling, taking place due to the extraordinary enhancement of the electromagnetic field inside the nanogap, results in the change of the nanoantenna coupling from the capacitive to the conductive one. As a result, the absorption-to-scattering ratio of the dimer significantly changes. Particularly, the scattering cross-section decreases by about three times, whereas the normalized absorption rises from about 12 to 18 with noticeably broadening of the spectral line.

https://doi.org/10.46991/PYSU:A/2023.57.3.101

MSC2020: Primary: 78A45; 78A50; 78A60.

Keywords: electron tunneling, nanorods, absorption, scattering, field enhancement.

Introduction. Metal nanoparticles exhibit tunable physicochemical properties when exposed to electromagnetic radiation. An external field forces conduction band electrons in metals to oscillate. These collective oscillations in turn excite localized surface plasmon waves, which resonate at specific incident frequencies, conditioned by the nanoparticle size, composition, geometry, material and the surrounding environment. Such resonances, termed localized surface plasmon resonances (LSPR), can lead to significant confinement of electromagnetic waves in nanoscale dimensions and dramatic increase of light intensity in the close surroundings of the nanoparticles [1,2].

With the development of nanofabrication technologies, it has become feasible to create more complex and advanced nanostructures. A plethora of nanostructures with different morphology, composition and arrangement, including individual

* E-mail: davit.manukyan@ysu.am

homogeneous nanoparticles [3], core-shells [4, 5], dimers [6, 7], trimers [8] and nanoplasmonic aggregate structures [2, 9] have been studied. Due to the plasmonic coupling of nanoparticles in such structures, an even greater field enhancements were demonstrated [2, 10]. Besides electromagnetic field enhancement, LSPR also produces a significant increase in scattering and absorption capabilities of the nanostructures.

Such magnificent properties naturally make nanostructures the subject of persistent research efforts. They have been widely adopted in different areas, including solar-energy conversion, photocatalysis, nanomedicine [2], and surface enhanced Raman scattering (SERS) sensors, where utilizing LSPR phenomenon has enabled remarkable enhancement of the naturally weak Raman scattering by orders of magnitude, allowing even single molecules to be detected [11]. In nonlinear optics, the electromagnetic near-field enhancements, caused by the LSPR, can also lead to increased nonlinearities in the surrounding medium of the nanoparticle. This effect can be used in all optical control of light absorption and scattering, where the propagation of the signal beam can be impacted and modified by changing the dielectric properties of propagation medium with a control beam [12]. Lastly, plasmonic systems allow for ultrafast processing of light, due to their ability to react to external stimuli on the timescale of several femtoseconds [13].

Among various topologies, nanodimers, consisting of two metal nanoparticles separated by dielectric nanogap, are of particular interest. Classical theory predicts arbitrarily large plasmonic capacitive coupling between nanoparticles, as long as the gap size is greater than zero. However, the classical approach does not take into account the quantum effects, which can deeply affect the plasmonic response of the nanostructure. Intense electromagnetic fields can cause electron tunneling effects to take place in subnanometer gaps, effectively changing the interaction mechanism between the nanoparticles and limiting the maximum obtainable field enhancement [7, 14].

In this paper, a nanoparticle dimer, consisting of two cylindrical nanoantennas is numerically studied. We analyze the scattering and absorption characteristics of the dimer, as well as the electromagnetic field enhancement taking place in subnanometer interparticle gap, in both capacitively- and conductively- coupled regimes. Section 2 describes the geometry of the system and the theoretical details of the simulation. In section 3, we provide the parameters of the simulation, as well as discuss the obtained results.

Geometry and Modeling. The schematics of the considered nanoantenna dimer as well as the zoomed area of subnanometer gap are depicted in Fig. 1, a. Two cylindrical nanoantennas with length L and radius r are oriented along y axis and separated by an air gap of width g. The bases of nanoantenas form semispheres with the same radius r. Whole system is surrounded by air, with the outmost boundary layers set as perfectly matched layer to ensure absence of back-scattered signals. The system is illuminated with a plain wave, polarized along y axis and propagating along x axis. The nanorods are made of gold, with the wavelength-dependent refractive index taken from [15]. One of the major ways of metallic nanoparticles

synthesis is the chemical synthesis, particularly the seed-mediated method, which allows for effectively smooth nanorods fabrication [16]. In addition, the surface roughness has negligible impact on the absorption and scattering characteristics of nanoparticles [17]. Chosen geometry and dimensions of Au nanoantennas result in the localized surface plasmon resonance appearing in the near infrared spectrum. On the other hand, subnanometer dimensions of the gap cause strong field enhancement. Sufficiently large electric field in the nanogap (of the order of $\sim 10^9\ V/m$) can cause the conduction electrons of the nanoantennas to overcome the quantum barrier of Au-air interface [18], hence quantum tunneling can occur, leading to electron channel between nanoantennas, schematically illustrated in Fig. 1, a by a semitransparent red region. This channel is represented by a cylinder with a radius of r_t, which is much smaller than the nanorod radius. The channel electrons yield changes in the effective dielectric permittivity $\varepsilon_{g,eff}$ of the insulating gap which is expressed as follows:

$$\varepsilon_{g,eff} = \varepsilon_r + i\sigma/(\omega\varepsilon_0) \tag{1}$$

where ε_r is the relative permittivity, $\varepsilon_0 = 8.85 \cdot 10^{-12}\ F/m$ is the vacuum permittivity, σ is the DC conductivity, $\omega = 2\pi f$ is the angular frequency and f is the excitation frequency. We assume ε_r to be equal to 1, matching the background medium. To simulate the tunneling effect we varied the conductivity of the tunneling region σ from 0 to $10^4\ S/m$, which corresponds to the theoretically suggested values for the given gap width [18].

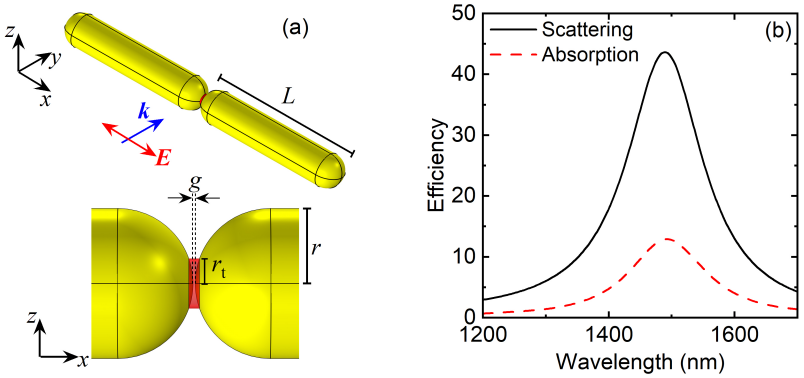

Fig. 1. a) The schematic view of the studied system, where L is the nanoantenna length, r is the nanoantenna radius, r_t is the gap radius, g is the gap width, E shows the incident field polarization, k is the wave vector; b) the dependency of scattering and absorption efficiencies on incident wavelength. $L = 230\ nm$, $r = 15\ nm$, $r_t = 4\ nm$, $g = 0.5\ nm$ were chosen as the geometrical parameters in this case. These values remain unchanged throughout the analysis if not otherwise stated.

In the following analysis we normalized the scattering and absorption cross-sections to the longitudinal geometrical cross-section of the nanoantenna dimer. The resulting unitless quantities are called scattering and absorption efficiencies, respectively. Throughout entire analysis the tunneling region and nanoantenna radii as well as the gap width are kept constant and equal to 4 nm, 15 nm, 0.5 nm, respectively.

Results and Discussion. For the plasmon resonance to be in near infrared spectrum we take the nanoantennas length $L = 230$ *nm*. Numerical analysis based on the finite element method (FEM) was conducted, to study the scattering and absorption capabilities of the system. The FEM is a popular analysis method, which discretizes the system by dividing it into smaller parts, called finite elements. Then the wave equation is solved for all of the finite elements, taking into account the boundary conditions. These simple equations that model the finite elements are then assembled into a system of equations, that models the entire problem. The FEM then approximates the solution by minimizing the error function via the calculus of variations [19] .

The dependence of the scattering and absorption efficiencies of the nanoantenna dimer with $L = 230$ *nm* on the incident wavelength is depicted in Fig. 1, b. The LSPR peak of such a system is around ~ 1500 *nm* wavelength, with scattering and absorption efficiencies reaching up to ~ 45 and ~ 13, respectively.

To demonstrate the tunability of the resonance wavelength we considered nanoantennas with three different lengths of $L = 180$ *nm*, 230 *nm* and 260 *nm*. The scattering (left axis) and absorption (right axis) efficiencies of these nanoantennas as a function of the incident wavelength are compared in Fig. 2, a. One can see that the resonance wavelength increases with the increase in nanoantennas length, ranging from ~ 1300 *nm* for 180 *nm* long antennas, to ~ 1600 *nm* for 260 *nm* long antennas. Longer nanoantennas also result in a slight increase in the resonant values of the absorption and scattering efficiencies.

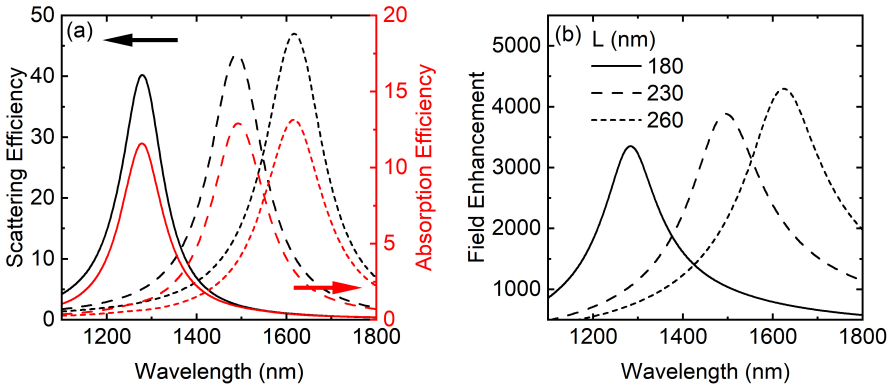

Fig. 2. The dependencies of (a) scattering and absorption efficiencies; (b) field enhancement on incident wavelength for $L = 180$ *nm*, 230 *nm*, 260 *nm* nanoantenna lengths. The legends in (b) also apply to (a). Everything else is as in Fig. 1.

Fig. 2, b shows the dependence of the electric field enhancement in the nanogap on the incident wavelength for the three considered lengths of nanoantennas. To evaluate field enhancement, we take the ratio of the electric field magnitude at the mass center of the nanogap to the incident wave field. For 180 *nm* long antennas the field enhancement value at resonance reaches up to ~ 3300. Increasing the

nanoantennas length results also in an increase in field enhancement peak values, reaching up to ~ 4300 for $L = 260$ *nm* nanoantennas. This can be explained using an analogy with a capacitor. The field strength in a capacitor is directly proportional to the voltage within the plates, which in turn is proportional to the amount of charge on capacitor plates. Here the dimer acts as a nanocapacitor, with nanoantennas being its plates. The longer the nanoantennas, the greater the number of free charges it is possible to accumulate at the semispherical edges of nanoantennas. In [20], it is shown that only a segment of the nanoantenna semispherical edge contributes to the capacitive coupling of nanoantennas. The gap channel radius r_t is picked according to this segment size.

Up to this point, we were considering the low incident intensity regime, where no effects related to the quantum tunneling occur. However, increasing the incident intensity will result in a formation of conductive channel between nanoantennas, with effective dielectric permittivity expressed according to the relation (1). To analyze the impact of the conductive channel on the optical response of the nanoantenna dimer, we consider three different cases, with channel conductivity of $\sigma = 0, 10^3\ S/m$, $10^4\ S/m$ (Fig. 3).

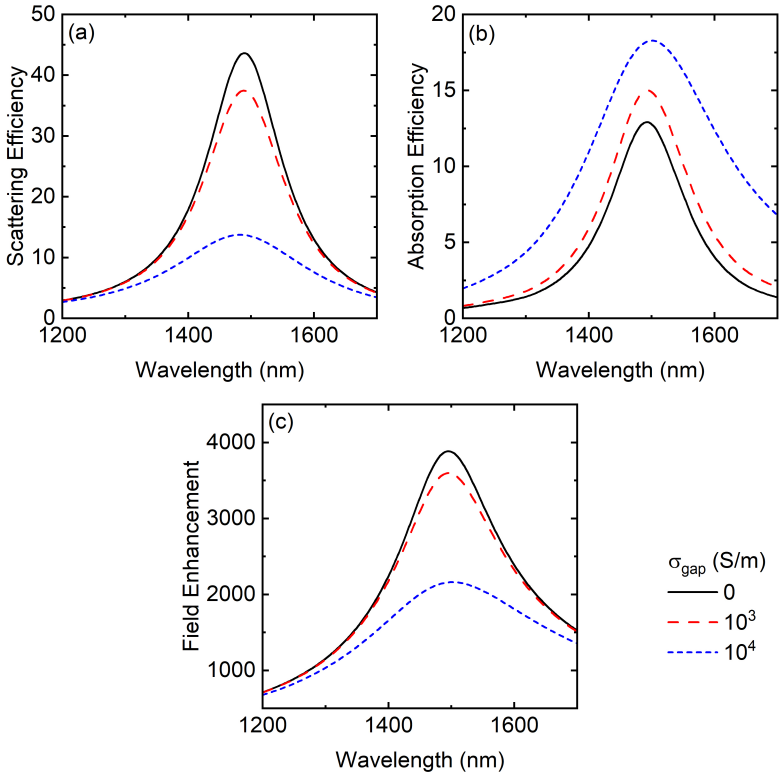

Fig. 3. Resonance plots for (a) scattering efficiency, (b) absorption efficiency and (c) field enhancement of the system with 230 *nm* cylindrical rods for $\sigma = 0\ S/m$, $10^3\ S/m$, $10^4\ S/m$ gap conductivity. Everything else is as in Fig. 1.

Fig. 3 depicts the dependence of the (a) scattering efficiency, (b) absorption efficiency and (c) field enhancement on the incident wavelength for different gap channel conductivity values. At the resonance wavelength the scattering efficiency decreases from ~ 45 to ~ 13 as the channel conductivity raises from $\sigma = 0\ S/m$ to $\sigma = 10^4\ S/m$. Analogously, the field enhancement in the gap also decreases from ~ 3900 for $\sigma = 0\ S/m$ to ~ 2200 for $\sigma = 10^4\ S/m$. On the other hand, the absorption efficiency increases as the gap channel conductivity increases, spanning from ~ 12.5 for $\sigma = 0\ S/m$ to ~ 18 for $\sigma = 10^4\ S/m$. Besides that, as the gap conductivity rises, one can also observe an increase in the absorption efficiency curve width, which is a consequence of the increase in the system losses. The absorption-to-scattering ratio in the linear regime at the resonance equals to approximately 0.3, whereas for $\sigma = 10^4\ S/m$ it increases up to ~ 1.33.

To reveal the overall influence of the channel conductivity on both efficiencies and the nanogap field enhancement, we fixed the incident wavelength at the resonance value for each of the three considered nanoantenna lengths (i.e. $\lambda = 1280\ nm$ for $L = 180\ nm$, $\lambda = 1490\ nm$ for $L = 230\ nm$ and $\lambda = 1620\ nm$ for $L = 260\ nm$) and swept the conductivity value from 0 to $10^4\ S/m$ (Fig. 4).

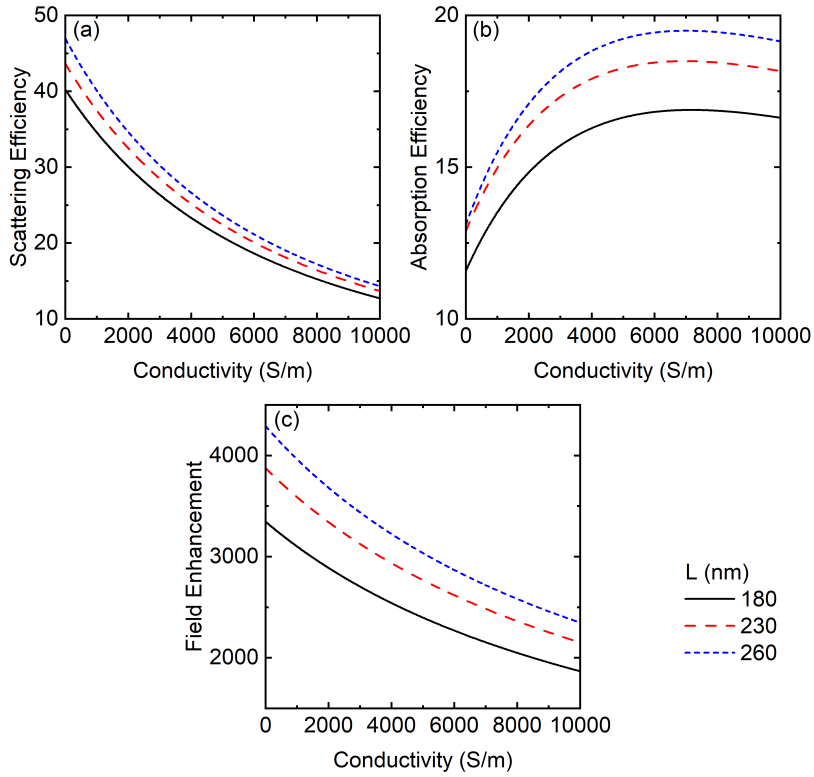

Fig. 4. The dependencies of (a) scattering efficiency, (b) absorption efficiency and (c) field enhancement from the gap conductivity for $L = 180\ nm$, $230\ nm$, $260\ nm$ nanoantenna lengths. Everything else is as in Fig. 1.

The imaginary part of the gap dielectric permittivity is ~ 0.9 for $\sigma = 10^4\ S/m$ and $\lambda = 1490\ nm$. Fig. 4, a shows that the scattering efficiency decreases almost three times with the increase in the gap channel conductivity, ranging from ~ 45 for $\sigma = 0\ S/m$ to ~ 15 for $\sigma = 10^4\ S/m$. On the contrary, the absorption efficiency noticeably increases as the channel conductivity raises and reaches its maximum value at $\sigma \approx 6.6 \cdot 10^3\ S/m$ (Fig. 4, b). Analysis of the absorption of electromagnetic waves by subwavelength particles shows that for small values of dielectric permittivity, there is a resonance of the absorption cross-section as a function of the imaginary part of dielectric permittivity [21]. As for the gap field enhancement, Fig. 4, c demonstrates almost twofold decrease in its value, which was expected since the tunneling effect in the gap acts as a negative feedback loop, leading to the reduction of the gap field.

This study presents a simplified model, which allows one to get an intuitive understanding about the optical characteristics of nanoantenna dimers under intense electromagnetic radiation, in which unique phenomena take place as a result of the switching between capacitive and conductive couplings of nanoantennas. This model will facilitate the discovery of the characteristics of the electromagnetic field control with the help of nanoantennas.

Conclusion. In summary, we have analyzed the scattering and absorption characteristics of nanoantenna dimers, exposed to external electromagnetic radiation. Considering a nanorod dimer with total length of 460 *nm* and the gap width of 0.5 *nm* we calculated the scattering and absorption efficiencies, as well as the field enhancement in the gap between nanoantennas. First we studied the low-intensity regime, where no electron tunneling occurs and derived the linear optical response of the dimer. The plasmon resonance of the system was observed at $\sim 1500\ nm$ wavelength, with scattering and absorption efficiencies, as well as field enhancement reaching up to ~ 45, ~ 13 and ~ 3900, respectively.

We further considered the high-intensity regime, where different electromagnetic phenomena take place. Strong incident waves resulted in a formation of a conductive channel between the nanoantennas due to electron tunneling. We fixed the incident wavelength at the resonance value and swept the gap channel conductivity from 0 to $10^4\ S/m$. The calculations show a decrease in scattering efficiency and field enhancement, whereas the absorption efficiency was increased.

The presented system can aid the investigation of the electromagnetic radiation impact on nanoparticle dimers and the implementation of all optical control of scattering and absorption.

I would like to express my gratitude to Prof. Kh. Nerkararyan and Dr. H. Parsamyan for the guidance and support provided to me throughout this research work.

Received 12.09.2023
Reviewed 05.11.2023
Accepted 11.11.2023

REFERENCES

1. Liz-Marzán L.M., Murphy C.J., Wang J. Nanoplasmonics. *Chem. Soc. Rev.* **43** (2014), 3820.
   https://doi.org/10.1039/c4cs90026j
2. Kasani S., Curtin K., Wu N. A Review of 2D and 3D Plasmonic Nanostructure Array Patterns: Fabrication, Light Management and Sensing Applications. *Nanophotonics* **8** (2019), 2065–2089.
   https://doi.org/10.1515/nanoph-2019-0158
3. Li B., Zu Sh., et al. Single-Nanoparticle Plasmonic Electro-Optic Modulator Based on MoS_2 Monolayers. *ACS Nano* **11** (2017), 9720–9727.
   https://doi.org/10.1021/acsnano.7b05479
4. Liu P., Chen H., et al. Fabrication of Si/Au Core/Shell Nanoplasmonic Structures with Ultrasensitive Surface-Enhanced Raman Scattering for Monolayer Molecule Detection. *J. Phys. Chem. C* **119** (2015), 1234–1246.
   https://doi.org/10.1021/jp5111482
5. Frost R., Wadell C., et al. Core–Shell Nanoplasmonic Sensing for Characterization of Biocorona Formation and Nanoparticle Surface Interactions. *ACS Sensors* **1** (2016), 798–806.
   https://doi.org/10.1021/acssensors.6b00156
6. Downing C.A., Mariani E., Weick G. Radiative Frequency Shifts in Nanoplasmonic Dimers. *Phys. Rev. B* **96** (2017), 155421.
   https://doi.org/10.1103/PhysRevB.96.155421
7. Aguirregabiria G., Marinica D.C., et al. Role of Electron Tunneling in the Nonlinear Response of Plasmonic Nanogaps. *Phys. Rev. B* **97** (2018), 115430.
   https://doi.org/10.1103/PhysRevB.97.115430
8. Liu A.C.Y., Lloyd J., et al. Mapping Local Surface Plasmon Modes in a Nanoplasmonic Trimer Using Cathodoluminescence in the Scanning Electron Microscope. *Microsc. Microanal.* **26** (2020), 808–813.
   https://doi.org/10.1017/S1431927620000094
9. Sperling J.R., Macias G., et al. Multilayered Nanoplasmonic Arrays for Self-Referenced Biosensing. *ACS Appl. Mater. Interfaces* **10** (2018), 34774–34780.
   https://doi.org/10.1021/acsami.8b12604
10. Paria D., Zhang C., Barman I. Towards Rational Design and Optimization of Near-Field Enhancement and Spectral Tunability of Hybrid Core-Shell Plasmonic Nanoprobes. *Sci. Rep.* **9** (2019), 16071.
    https://doi.org/10.1038/s41598-019-52418-9
11. Sharma B., Frontiera R.R., et al. SERS: Materials, Applications, and the Future. *Mater. Today* **15** (2012), 16–25.
    https://doi.org/10.1016/S1369-7021(12)70017-2
12. Kauranen M., Zayats A.V. Nonlinear Plasmonics. *Nat. Photonics* **6** (2012), 737–748.
    https://doi.org/10.1038/nphoton.2012.244
13. Stockman M.I. Nanoplasmonics: Past, Present, and Glimpse into Future. *Opt. Express* **19** (2011), 22029.
    https://doi.org/10.1364/OE.19.022029
14. Esteban R., Zugarramurdi A., et al. A Classical Treatment of Optical Tunneling in Plasmonic Gaps: Extending the Quantum Corrected Model to Practical Situations. *Faraday Discuss.* **178** (2015), 151–183.
    https://doi.org/10.1039/C4FD00196F

15. Babar S., Weaver J.H. Optical Constants of Cu, Ag, and Au Revisited. *Appl. Opt.* **54** (2015), 477.
https://doi.org/10.1364/ao.54.000477
16. Halas N.J., Lal S., et al. Plasmons in Strongly Coupled Metallic Nanostructures. *Chem. Rev.* **111** (2011), 3913–3961.
https://doi.org/10.1021/cr200061k
17. Trügler A., Tinguely J.-C., et al. Influence of Surface Roughness on the Optical Properties of Plasmonic Nanoparticles. *Phys. Rev. B* **83** (2011), 081412.
https://doi.org/10.1103/PhysRevB.83.081412
18. Zhang P. Scaling for Quantum Tunneling Current in Nano- and Subnano-Scale Plasmonic Junctions. *Sci. Rep.* **5** (2015), 9826.
https://doi.org/10.1038/srep09826
19. Logan D.L. *A First Course in the Finite Element Method.* United Kingdom, Cengage Learning (2011) (Online).
https://books.google.am/books?id=KGZtCgAAQBAJ
20. Benz F., de Nijs B., et al. Generalized Circuit Model for Coupled Plasmonic Systems. *Opt. Express* **23** (2015), 33255.
https://doi.org/10.1364/OE.23.033255
21. Landau L.D., Pitaevskii L.P., Lifshitz E.M. *Electrodynamics of Continuous Media* (2nd ed.). United Kingdom, Oxford, Elsivier Sciences & Technology (1984).

Դ. Ա. ՄԱՆՈՒԿՅԱՆ

ՈՒԺԵՂ ԿԱՊՎԱԾ ՆԱՆՈՁՈՂԵՐԻ ՌԵԶՈՆԱՆՍԱՅԻՆ ԱՐՁԱԳԱՆՔԸ ԷԼԵԿՏՐԱՄԱԳՆԻՍԱԿԱՆ ԱԼԻՔԻՆ

Առանցքով միմյանց մոտ տեղադրված նանոձողերի էլեկտրամագնիսական արձագանքը կարող է կառավարվել դրանց միջև էլեկտրոնների թունելային անցմամբ պայմանավորված փոխազդեցության փոփոխությամբ: Ուսումնասիրվել է 230 *nm* երկարությամբ և միմյանցից առանցքի երկայնքով 0.5 *nm* հեռավորությամբ բաժանված, օդով շրջապատված նանոձողերից կազմված համակարգի օպտիկական արձագանքը արտաքին ուժեղ էլեկտրամագնիսական դաշտին: Վերջավոր տարրերի մեթոդի վրա հիմնված համակարգչային մոդելավորման միջոցով ցույց է տրվել, որ նանոձողերը բաժանող ենթանանոմետրական ճեղքում ձևավորվող էլէկտրամագնիսական դաշտի արտասովոր ուժեղացման հետևանքով առաջացող էլեկտրոնների թունելային անցումը փոփոխում է դրանց կապի բնույթը՝ ունակայինից հաղորդականայինի: Արդյունքում գրանցվում է համակարգի կլանման և ցրման փոխհարաբերակցության էական փոփոխություն: Մասնավորապես, ցրման կտրվածքը նվազում է մոտ 3 անգամ, մինչդեռ նորմավորված կլանումը աճում է մոտ 12-ից մինչև 18, սպեկտրային գծի նկատելի ընդլայնմամբ:

Д. А. МАНУКЯН

РЕЗОНАНСНЫЙ ОТКЛИК СИЛЬНО СВЯЗАННЫХ НАНОСТЕРЖНЕЙ НА ЭЛЕКТРОМАГНИТНУЮ ВОЛНУ

Электромагнитный отклик близко расположенных по оси наностержней можно контролировать изменением взаимодействия, обусловленным туннельным переходом электронов. Система состоит из двух золотых стержней длиной 230 *nm*, находящихся в воздухе и разделенных зазором шириной 0,5 *nm*. На основе метода конечных элементов выявлено, что туннельный переход электронов, возникающий из-за необычного усиления электромагнитного поля внутри нанозазора, приводит к изменению природы связи наноантенн – с емкостной на проводящую. В результате существенно меняется соотношение поглощения и рассеяния димера. В частности, сечение рассеяния уменьшается примерно в три раза, тогда как нормированное поглощение возрастает примерно с 12 до 18 при заметном расширении спектральной линии.